Statistical Optimization of the Synthesis of Highly Microporous Carbons by Chemical Activation of Kraft Lignin with NaOH

Vanessa Torné-Fernández,*[†] Josep María Mateo-Sanz,[†] Daniel Montané,[†] and Vanessa Fierro[‡]

Departament d'Enginyeria Química, Universitat Rovira i Virgili, Av. dels Països Catalans 26, E-43007 Tarragona, Spain, and Laboratoire de Chimie du Solide Minéral, Université Henri Poincaré-Nancy I, UMR-CNRS 7555, BP 239, 54506 Vandoeuvre-lès-Nancy, France

Highly microporous carbon materials with high apparent surface areas (up to 2400 $m^2 \cdot g^{-1}$) were obtained by heat treatment of mixtures of demineralized Kraft lignin and sodium hydroxide. The application of a statistical tool, the response surface methodology, was used to determine the optimum operation conditions for preparing activated carbon able to adsorb large quantities of organic compounds. For that purpose, three parameters were varied: temperature of activation, sodium hydroxide and demineralized Kraft lignin percent mass ratio, and nitrogen flow rate. This carbon was tested for the adsorption of methylene blue that is a model compound for the most usual organic pollutant behavior, such as dyes. The adsorption of methylene blue was 93.2 g/100 g activated carbon, and this has a high microporosity and a specific surface area of 2610 $m^2 \cdot g^{-1}$. The optimum preparation conditions of this best activated carbon were determined at 755 °C, 22.4 % Kraft lignin, and 200 cm^3 $N_2 \cdot min^{-1}$.

1. Introduction

Lignin is a biopolymer that may be obtained in large quantities as a byproduct during the chemical pulping of wood and annual plants for the production of cellulose pulps. Several technical lignins are available depending on the pulping process, such as Kraft lignin (KL), lingosulfonates, and organosolv lignin, the first being the most abundant. In the Kraft process, lignin is used as in-house fuel to supply energy to the process, which also allows the simultaneous regeneration of the pulping chemicals. However, the enormous amount of lignin that is processed yearly through Kraft pulping plants has prompted interest on finding higher value applications for this material. Some uses that have been explored are as binder for animal fodder, to prepare lubricants for oil well drilling, in soil stabilization, as a substitute for phenol in adhesives, and as a precursor to the manufacture of activated carbon. The latter is currently a favored application because the demand of carbonaceous adsorbents is growing worldwide driven by stricter environmental regulations, which force improvement in separation techniques and intensive processing of waste streams to reduce the emissions of gas and liquid contaminants. Activated carbons (AC) and carbon molecular sieves are used industrially for gas separation, gas storage, purification, and catalyst supports.[1,2] Properties of a carbonaceous adsorbent depend on the surface area, the pore volume distribution, and the chemistry of the surface. All of those factors are a direct consequence of the nature of the precursor material and, most importantly, on the activation agent and conditions.[3−8] In recent studies on the chemical activation of KL with H_3PO_4,[9,10] we obtained microporous AC with surface areas as high as 1300 $m^2 \cdot g^{-1}$, although higher specific surfaces may be obtained with other activating agents. There is a growing interest in activation with alkaline hydroxides, and potassium hydroxide (KOH) has been found to be one of the most effective compounds for that purpose.[8,11−14] High surface areas and pore volumes are reported for lignocellulosic materials, carbons, and chars activated by KOH, with surface areas up to 3000 $m^2 \cdot g^{-1}$.[15] Exploratory studies evidenced the possibility of preparing highly microporous carbons from KL using sodium hydroxide (NaOH) and KOH as an activating agent under suitable experimental conditions.[15]

Therefore, the aim of the present work was to develop a systematic study to optimize the manufacture of AC from KL by activation with NaOH from the effect of the operating variables on the characteristics of the resulting carbon. A statistical design based on the response surface methodology (RSM)[16−24] has been developed to optimize the capacity for methylene blue adsorption (q_{MB}) because it serves as a model compound for the most usual organic pollutants.[15,17,25−37] Iodine number is another relative indicator of the AC porosity but in general terms is not as useful as methylene blue to predict the AC ability for adsorption of other species.

2. Experimental Section

2.1. Materials. KL was supplied by Lignotech Ibérica S.A. (Spain) and was presented in the form of a fine dark-brown powder. Ash content of the lignin was 9.5 % on reception, and lignin was demineralized prior to the preparation of the carbon.[38] To remove the inorganic matter from KL, batches of 100 g were introduced in 2 L of water, leading to dark-brown suspensions of pH 9.5, and lignin was then precipitated by the addition of H_2SO_4 until the pH decreased to 1. The precipitate was gently washed with distilled water until constant pH, and it was dried overnight at 105 °C. Lignin prepared this way was nearly mineral-free and was labeled demineralized KL (KL_d).

Extra pure methylene blue chloride (MB) powder was supplied by Scharlau and used as a solution of 3.2 mM concentration with 5 % HNO_3. MB serves as a model compound

---

* Corresponding author. E-mail: vanessa.torne@urv.cat. Tel: + 34 977 558 577. Fax: + 34 977 559 621.
[†] Universitat Rovira i Virgili.
[‡] Université Henri Poincaré.

10.1021/je800827n CCC: $40.75

Table 1. Physical and Chemical Properties of the Commercial Activated Carbons

property	CAC1	CAC2	CAC3
S_{BET} ($m^2 \cdot g^{-1}$)	1350	620	1020
$V_{\alpha,micro}$ ($cm^3 \cdot g^{-1}$)	0.458	0.185	0.334
$V_{\alpha,ultra}$ ($cm^3 \cdot g^{-1}$)	0.139	0.085	0.152
$V_{0.99}$ ($cm^3 \cdot g^{-1}$)	0.713	0.637	0.625
acidic groups (mequiv H^+/g_{AC})	2.6	7.9	5.0
basic groups (mequiv OH^-/g_{AC})	0.5	1.2	2.1
q_{MB} (g MB/100 g CAC)	41.5	31.5	21.7

for adsorption of organic contaminants from aqueous solution, and it is used as a primary indicator of the adsorption capacity of Acs (q_{MB}).[17]

NaOH of 99 % purity was purchased in the form of lentils from Scharlau.

2.2. Preparation of the Activated Carbon. NaOH lentils were ground and physically mixed with KL_d at KL_d-to-total-mix mass ratios (R) between 18 % and 32 %. The carbonization was carried out in a horizontal tubular furnace, where the samples were heated in a crucible at 5 °C·min^{-1} from room temperature to a nominal carbonization temperature (T_{carb}) between (700 and 869) °C. A flow of N_2 (f) between (200 and 500) cm^3·min^{-1} was used, and the samples were kept at T_{carb} for 1 h before they were cooled under a nitrogen atmosphere.

During the experiments, metallic sodium mixed with sodium carbonate was present. Therefore, the AC was submitted to atmospheric humidity for 1 day to oxidize sodium metal slowly and was washed with extreme care, first with 1 M HCl and finally with distilled water until a constant pH of around 6. After drying in an oven during 24 h, a very light activated carbon was obtained.

q_{MB} of the carbons prepared from KL was compared with that of three commercial AC (CAC1, CAC2 and CAC3), which were kindly provided by Norit Americas. These carbons are prepared by physical activation with steam, and their main properties are shown in Table 1. CAC1 (Norit PAC200) and CAC3 (Norit ROX 0.8) are mainly microporous with high surface areas of more than 1000 m^2·g^{-1}. CAC2 (DARCO 12X40) has a lower surface area and is less than 30 % microporous (0.185 cm^3·g^{-1} in microporous volume with respect to a total volume of 0.637 cm^3·g^{-1}). All of them have an acidic surface character.

2.3. Response Surface Methodology. Experiments were planned using a RSM, which was based on a factorial design around a central point located in the expected optimal zone (Figure 1).[39,40] q_{MB} was chosen to be the dependent variable, and the independent variables were R, T_{carb}, and f.[15] Figure 2 shows the algorithm followed in the RSM. Analysis of the RSM determined the significance of the effect of the independent variables and their interactions. The design was further expanded with a second set of experiments into a compost central factorial design (Figure 2) to locate the optimum more precisely.

2.4. Characterization of the Activated Carbons. Surface area and porosity were determined by the application of different methods to the nitrogen adsorption−desorption isotherms obtained at 77 K in a Micromeritics ASAP 2020 analyzer. The samples were previously degassed at 523 K for several hours. N_2 adsorption−desorption data were analyzed according to: (i) the BET method[41] for calculating the specific surface area, S_{BET}; (ii) the α_S method[42] for calculating the micropore ($V_{\alpha,micro}$) and the ultramicropore ($V_{\alpha,ultra}$) volumes, using Carbopack F graphitized carbon black as reference material.[43] The total pore volume, $V_{0.99}$, was calculated from nitrogen adsorption at a relative pressure of 0.99.

The test for MB adsorption (q_{MB}) is based on one point of experimental adsorption equilibrium. Analysis was performed by triplicate mixing of 33.7 mg of AC with 50 mL of a solution of 3.2 mM MB. This suspension remained under mechanical stirring for 24 h. Afterward, a sample of the solution was extracted, and we determined the concentration of MB by measuring its absorbance at 664.8 nm in a Dinko Instruments 8500 spectrophotometer. q_{MB} was calculated by the difference between the initial and the final concentrations and was expressed as grams of MB per 100 g of AC (g_{MB}/100 g_{AC}). The error concerning this measure is less than 0.5 %, and it comes from the equipment used.

A modification of the Boehm titration[44] was used to quantify the acidic and basic surface groups. Dry samples of AC (25 mg) were mixed with 25 mL of 0.1 N NaOH, 0.1 N Na_2CO_3, 0.1 N $NaHCO_3$, 0.1 N sodium ethoxide, or 0.05 N HCl. The first four solutions measure the acidic surface sites whereas the latter is used to quantify the total basic sites. NaOH is used to quantify carboxylic, lactone, and phenol groups; Na_2CO_3 is used to quantify carboxylics and lactones; and $NaHCO_3$ determines carboxylics and sodium ethoxide for the total acidic sites. The suspensions of AC were stirred for 48 h to ensure complete contact between the surface groups and the reagent in the solution. Afterward, the suspension was filtered, and a sample of 5 mL was titrated with HCl or NaOH, depending on the solution. Total titrable surface functional groups were expressed in terms of milliequivalents per gram of AC (mequiv/g_{AC}).

Conversion to AC (η) is the carbon yield calculated as the coefficient between the final dry weight of the carbon and the initial demineralized lignin weight. The error concerning to this measure is the error of the balance ($6 \cdot 10^{-04}$).

3. Results and Discussion

3.1. Application of Response Surface Methodology to Optimize Adsorption Capacity. In a preliminary study on the preparation of AC with KL_d and NaOH,[16] it was established that T_{carb}, R, and f were the variables that had the most significant effect on the yield and properties of AC, whereas the activation time and the heating rate had less effect.[45] For this reason, we set the activation time and the heating rate for all experiments to be 1 h and 5 °C·min^{-1}, respectively.

3.1.1. First Screening Experiments. A first set of 17 ACs was prepared following the central factorial design under the conditions detailed in Table 2, for the simple analysis, and Table 3, for the compost analysis, and their conversion to AC (η) and q_{MB} was measured. The central point was fixed at 770 °C (T_{carb}), 25 % (R), and 350 cm^3·min^{-1} (f) according to previous work.[6,46−50] Analysis of the results (Table 3) shows: (i) below 770 °C, q_{MB} has a moderate decrease when the KL_d mass ratio increases at a constant temperature; (ii) above 770 °C, a decrease in the KL_d mass ratio produces an important decrease in the q_{MB} because the structure of the AC begins to collapse, causing the specific surface area of the carbon to fall;[15] (iii) a maximum in MB adsorption was always observed around 770 °C at constant R.

Table 4 presents the statistical analysis of the central factorial design obtained by the RSM of the results from Table 2. The probability of each variable to influence the q_{MB} in the linear and quadratic approximations of the RSM is reported. At a 95 % probability level, a p-value below 0.050 means that this parameter has a significant influence, and p-values near 0.100 mean that the parameter has some influence.

Application of a linear approximation gave information about the influence of T_{carb}, R, and f, on the MB adsorption. Table 4

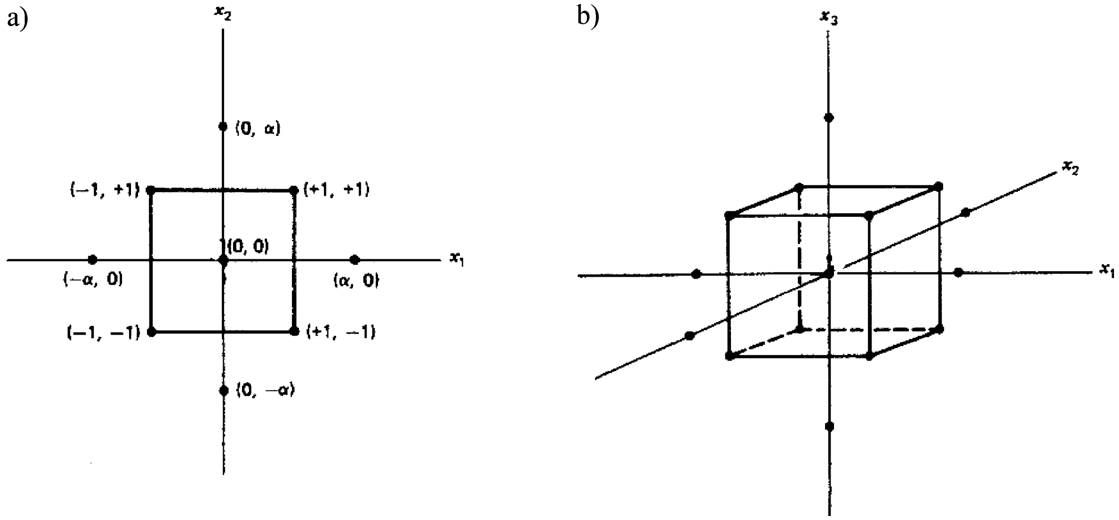

Figure 1. Scheme of experimental points for the response surface method (RSM) with (a) two independent variables and (b) three independent variables.

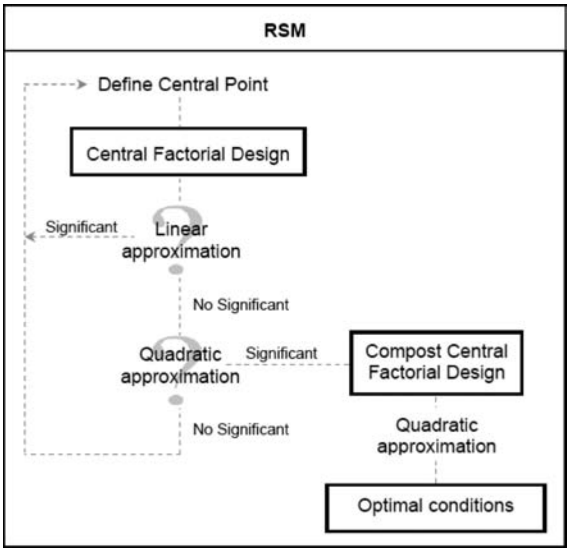

Figure 2. Procedure of the response surface method.

Table 3. Compost Central Factorial Design Points Studied in the First-Step Experiments

	real values			codified values		
experiment	T_{carb} (°C)	R (%)	η (%)	T_{carb}	R	q_{MB} (g/100 g_{AC})
1, 11	700	20		−1	−1	83.1
2, 10	840	20		1	−1	44.3
3	770	25	20.9	0	0	86.7
4, 7	840	30		1	1	83.7
5, 8	700	30		−1	1	73.1
6	770	25	21.0	0	0	90.8
9	770	25	21.0	0	0	91.8
			axial points			
12	770	32	31.8	0	$\sqrt{2}$	91.5
13	869	25	19.6	$\sqrt{2}$	0	91.9
14	770	25	24.5	0	0	96.1
15	770	25	23.0	0	0	94.7
16	671	25	26.6	$-\sqrt{2}$	0	77.0
17	770	18	6.6	0	$-\sqrt{2}$	83.4

shows that the three parameters of the linear approximation have p-values above 0.200. It means that these parameters do not have a significant linear effect on the adsorption of the MB. However, comparison among them shows that T_{carb} and R appeared to be more important than f. Results from the quadratic approximation of the central factorial design show that the experiments were well represented by the quadratic surface approximation because the p-value for $(T_{\text{carb}}^2 + R^2 + f^2)$ was below 0.050. f and its interaction effects with T_{carb} and R gave p-values above 0.309; therefore, f was determined to not be a significant variable, and a constant value of 200 $\text{cm}^3\ \text{N}_2\cdot\text{min}^{-1}$ [6,50,51] was maintained for the rest of the study. In contrast, the influences of T_{carb} and R on the adsorption of MB were not strictly significant at 95 % probability, but their respective p-values, 0.084 and 0.078, were close to 0.05. Furthermore, the p-value of their interaction effect was below 0.050, which indicates that both variables may really have a significant effect.

Therefore, from the results obtained with the experiments of Table 2, the central factorial design has been explained to be a compost central factorial design (Table 3) omitting the independent variable f. Values of Table 3 have been obtained from

Table 2. Central Factorial Design Points Studied in the First-Step Experiments

	real values				codified values			
experiment	T_{carb} (°C)	R (%)	f ($\text{cm}^3\cdot\text{min}^{-1}$)	η (%)	T_{carb}	R	f	q_{MB} (g/100 g_{AC})
1	700	20	200	19.7	−1	−1	−1	79.2
2	840	20	500	21.4	1	−1	1	38.7
3	770	25	350	20.9	0	0	0	86.7
4	840	30	200	27.8	1	1	−1	85.1
5	700	30	500	26.6	−1	1	1	62.6
6	770	25	350	21.0	0	0	0	90.8
7	840	30	500	21.7	1	1	1	82.2
8	700	30	200	30.4	−1	1	−1	83.6
9	770	25	350	21.0	0	0	0	91.8
10	840	20	200	6.3	1	−1	−1	49.8
11	700	20	500	12.6	−1	−1	1	87.0

Table 4. Statistical p-Value for the Simple and the Compost Central Factorial Design in the First-Step Experiments

central factorial design	approximation	linear effect T_{carb}	linear effect R	linear effect F	interaction effect $T_{carb}\cdot R$	interaction effect $T_{carb}\cdot f$	interaction effect $R\cdot f$	quadratic effect $T_{carb}^2 + R^2 + f^2$	quadratic effect T_{carb}^2	quadratic effect R^2
simply	linear	0.299	0.282	0.606						
	quadratic	0.084	0.078	0.309	0.021	0.974	0.423	0.039		
compost	quadratic	0.825	0.229		0.059				0.114	0.191

Table 5. Points Studied in the Second-Step Experiments

experiment	real values T_{carb} (°C)	real values R (%)	η (%)	codified values T_{carb}	codified values R	q_{MB} (g/100 g_{AC})
18	807	25	18.4	1	1	93.2
19	747	21	15.1	−1	−1	94.3
20	777	23	19.0	0	0	96.2
21	807	21	6.8	1	−1	91.9
22	747	25	22.2	−1	1	94.1
23	777	23	18.6	0	0	94.2
24	777	23	13.7	0	0	95.4
			axial points			
25	777	20	10.5	0	$-\sqrt{2}$	95.1
26	777	26	19.0	0	$\sqrt{2}$	88.0
27	777	23	18.9	0	0	95.4
28	777	23	17.5	0	0	94.6
29	777	23	17.0	0	0	95.7
30	819	23	14.1	$\sqrt{2}$	0	90.3
31	735	23	17.5	$-\sqrt{2}$	0	95.7

Table 6. Statistical p-Value Analysis of the Data Presented in Table 5

central factorial design	approximation	linear effect T_{carb}	linear effect R	interaction effect $T_{carb}\cdot R$	quadratic effect $T_{carb}^2 + R^2$	quadratic effect T_{carb}^2	quadratic effect R^2
simply	linear	0.326	0.728				
	quadratic	0.243	0.640	0.534	0.133		
compost	quadratic	0.068	0.123	0.693		0.170	0.033

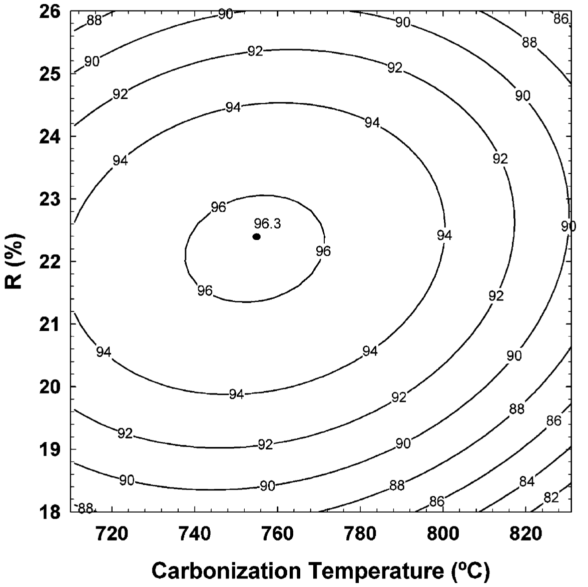

Figure 3. Variation of the quantity of MB adsorbed depending on the temperature (T) and the KL_d quantity (R).

the average of the data with equal T_{carb} and R but different f of Table 2 and the experiments in the axial points.

Table 4 also presents the statistical analysis for the compost central factorial design for T_{carb} and R of Table 3 by the RSM, where the probability of each variable to influence the q_{MB} in the quadratic approximations of the RSM is reported. All parameters are above 0.050, although, there are indications of the quadratic influence of the independent variables T_{carb} and R due to the p-values (0.114 and 0.191, respectively). However, some interaction of these two variables is observed with a p-value of 0.059. Therefore, a quadratic function was adjusted with data of Table 3, and a maximum q_{MB} was obtained at 900 °C (T_{carb}) and 37 % (R). These conditions were localized out of the defined working conditions range and were contradictory with those expected due to a large range of studies obtaining AC under extreme conditions that collapse the structure and thus low adsorption capacities that, in the case studied, generate distortions in the data analysis.

3.1.2. Experiments with a Redefined Central Point. Because f was not a significant variable but the significance of T_{carb} and R was not clearly established and the optimum was not located, a second set of experiments was conducted around a new central point, which uses smaller variations. The central point was fixed at 777 °C (T_{carb}) and 23 % (R), and variations of ± 30 °C and ± 2 % were employed for the experimental design.

Fourteen new samples of AC were prepared under the conditions detailed in Table 5, and their q_{MB} values were measured. Statistical analysis of experimental data of Table 5 for the RSM gave the p-values reported in Table 6. Simple central factorial design presents the fact that both p-values in the linear approximation are above 0.300, showing no significant linear effect in the adsorption of the MB. Nevertheless, a comparison of them shows that T_{carb} seems to have a higher linear effect than R. Results from the quadratic approximation indicate that the influence of both parameters independently, 0.243 (T_{carb}) and 0.640 (R), and their combined effect, 0.534 ($T_{carb}\cdot R$), were not all significant, but the data can be represented by the quadratic surface approximation ($T_{carb}^2 + R^2 = 0.133$), and the compost central factorial design can be performed. The p-value of the quadratic effect is 0.133 caused by the dispersion of q_{MB} data in the central point. Therefore, compost central factorial design must be done because the probability level is near to 95 % and the average q_{MB} of the central points is higher than that obtained in the extremes of the range studied.

In the compost central factorial design, linear effect is significant with p-values of T_{carb} and R near 0.100 (Table 6) with a higher effect of the temperature, as is predicted in the central factorial design. Influence of the interaction between the two parameters is not clear, but the quadratic effect is important (Table 6, $T_{carb}^2 = 0.170$ and $R^2 = 0.033$), proving that the quadratic surface should give the optimum conditions to prepare an AC with maximum q_{MB} in this zone.

Figure 3 shows the RSM model locating an optimum AC prepared at 200 $cm^3\ N_2\cdot min^{-1}$, 755 °C, and 22.4 % in KL_d content with a predicted maximum of q_{MB} of 96.3 g MB/100 g_{AC}. However, the surface has little curvature around this optimum. Therefore, the maximum is located in the center of this range.

AC prepared under those optimal conditions has a q_{MB} of 93.2 g MB/100 g AC. Its specific surface area is 2612 $m^2\cdot g^{-1}$ with microporosity higher than 74 % (1.112 $cm^3\cdot g^{-1}$) of the total porosity (1.494 $cm^3\cdot g^{-1}$). Its surface was predominantly basic, with 16.6 $mequiv\cdot g^{-1}$ of basic groups and only 11.9 $mequiv\cdot g^{-1}$ of acidic groups, showing that surface chemistry also plays a main role in the MB adsorption. Comparing CAC with the optimum AC, q_{MB} is less than two times with respect to the optimum AC (41.5 g MB/100 g CAC1, 31.5 g MB/100

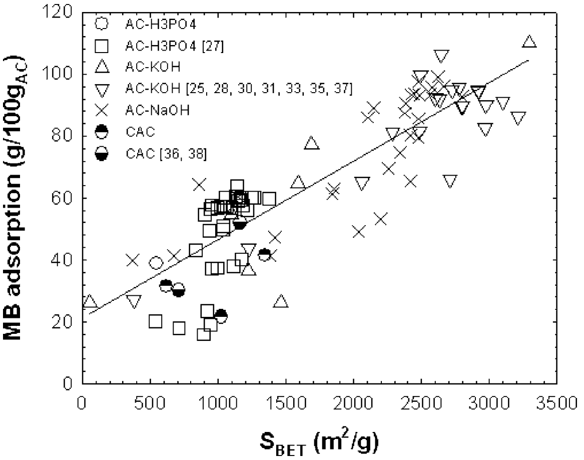

Figure 4. Evolution of the MB adsorption capacity with surface area for carbons obtained by chemical and physical activation. Continuous line only shows the general trend.

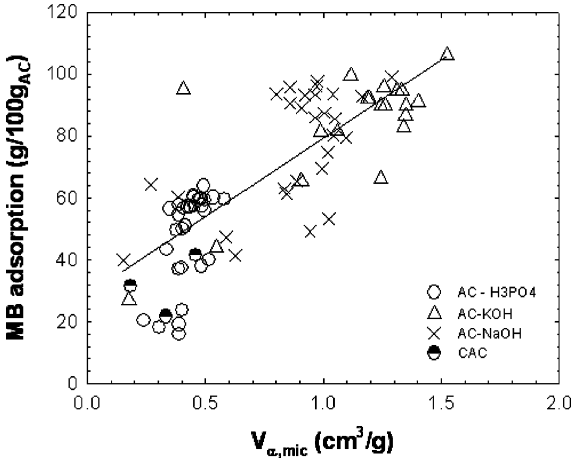

Figure 5. Evolution of the MB adsorption capacity with micropore volume for carbons obtained by chemical and physical activation. Continuous line only shows the general trend.

g CAC2, 21.7 g MB/100 g CAC3). Taking CAC1 properties for comparison with optimum AC properties shows that both microporosity and surface chemistry play an important role in MB adsorption.

Indeed, in some cases where the surface area and the porosity are less developed, the MB adsorption capacity is greater than expected and is caused by the surface chemistry.[25,52] MB is a dye with basic character, and when it is put in contact with a strong acid surface charge, electrostatic interactions act between the delocalized π electron of the carbon surface and the free electrons of the dye molecule that are principally present in aromatic rings.[52]

3.2. Dependency of the Methylene Blue Adsorption Capacity. In general, the q_{MB} of an AC is closely related to the specific surface area and especially to the microporosity in AC with highly microporous carbons with a significant contribution of narrow microporosity. Figure 4 shows the q_{MB} for ACs prepared by chemical and physical activation where carbons obtained by chemical activation include our own results on ACs from KL and KL$_d$ activated with H_3PO_4,[26] KOH,[15] and NaOH and bibliographic data on carbons prepared by activation with H_3PO_4,[27] KOH,[25,28,30,31,33,35,37] and steam.[34,36] Three CAC are also included. q_{MB} for the ACs prepared in this study range from (49.8 to 97.4) g MB/100 g AC, which is in good agreement with the results reported by several authors[25,30,31,33,35,37] for carbons prepared from different types of raw materials (olive stone, petroleum coke, pistachio shells, wood, etc.) by KOH activation (from (26.3 to 110.0) g MB/100 g AC), which lies in the same range of values as that for NaOH carbons. Large porosities and surface areas of the ACs prepared with NaOH and KOH facilitate the efficient adsorption of large quantities of adsorbates, and thus carbons can find application in removing organic and inorganic molecules from contaminated streams efficiently.[27,28,30,31,37] In contrast, ACs prepared from KL by phosphoric acid activation have more limited q_{MB}, about 38.9 g MB/100 g AC,[27] which is caused by the lower specific surfaces. Finally, carbons activated with steam[34,36] and the three CACs tested in this study have adsorption capacities similar to those of phosphoric acid carbons.

Because of the size of the MB molecule, around 15 Å, this compound is adsorbed only in larger micropores or supermicropores [(13 to 20) Å] and the mesopores (>20 Å). Figure 5 shows the variation of q_{MB} with the micropore, confirming that MB is adsorbed on them.

4. Conclusions

The aim of this study was to study the interaction between the preparation conditions of AC and experimental variables by using a statistical method for the design of experiments to produce optimized AC from KL activated with NaOH.

The statistical method selected, the RSM, has been shown to provide the optimum conditions for preparation of an AC that adsorbs more MB than the CAC used for comparison.

In the first step of the experimental application of the RSM, the effect of f and its interaction with T_{carb} and R was not significant and does not affect the final properties of the AC, especially the adsorption of MB. A typical constant value of 200 cm^3 $N_2 \cdot min^{-1}$ (f) was set for the remaining experiments centered in a second central point.

Integration of the first-step and the second-step experiments allowed us to select the optimum AC, where the maximum MB adsorption that takes place is achieved at 755 °C (T_{carb}), 22.4 % (R), and 200 cm^3 $N_2 \cdot min^{-1}$ (f) with a MB adsorption capacity of 96.3 g MB/100 g$_{AC}$. These adsorption capacities are well correlated with the supermicropore and mesopore volume and also with the acidic groups of the surface because of the character of the basic dye employed.

Note Added after ASAP Publication: This paper was published ASAP on May 18, 2009. V. Fierro was added as an author and the affiliations were updated. The revised paper was reposted on July 8, 2009.

Literature Cited

(1) *Activated Carbon Compendium : A Collection of Papers from the Journal Carbon 1996−2000*; Marsh, H., Ed.; Elsevier: North Shields, U.K., 2001.

(2) Lin, S. Y.; Lin, I. S. Lignin. In *Ullman's Encyclopedia of Industrial Chemistry*; Wiley: New York, 1990; Vol. A15, pp 305−315.

(3) Ahmad, A. L.; Loh, M. M.; Aziz, J. A. Preparation and characterization of activated carbon from oil palm wood and its evaluation on methylene blue adsorption. *Dyes Pigm.* **2007**, *75*, 263–272.

(4) Duran-Valle, C. J.; Gomez-Corzo, M.; Gomez-Serrano, V.; Pastor-Villegas, J.; Rojas-Cervantes, M. L. Preparation of charcoal from cherry stones. *Appl. Surf. Sci.* **2006**, *252*, 5957–5960.

(5) Ganan, J.; González, J. F.; González-García, C. M.; Ramiro, A.; Sabio, E.; Roman, S. Air-activated carbons from almond tree pruning: Preparation and characterization. *Appl. Surf. Sci.* **2006**, *252*, 5988–5992.

(6) Lillo-Rodenas, M. A.; Lozano-Castelló, D.; Cazorla-Amorós, D.; Linares-Solano, A. Preparation of activated carbons from Spanish anthracite. II. Activation by NaOH. *Carbon* **2001**, *39*, 751–759.

(7) Lozano-Castelló, D.; Cazorla-Amorós, D.; Linares-Solano, A.; Quinn, D. F. Influence of pore size distribution on methane storage at relatively

low pressure: preparation of activated carbon with optimum pore size. *Carbon* **2002**, *40*, 989–1002.
(8) Lozano-Castelló, D.; Lillo-Rodenas, M. A.; Cazorla-Amorós, D.; Linares-Solano, A. Preparation of activated carbons from Spanish anthracite. I. Activation by KOH. *Carbon* **2001**, *39*, 741–749.
(9) Fierro, V.; Torné-Fernández, V.; Montané, D.; Celzard, A. Study of the decomposition of Kraft lignin impregnated with orthophosphoric acid. *Thermochim. Acta* **2005**, *433*, 142–148.
(10) Fierro, V.; Torné-Fernández, V.; Montané, D.; Salvadó, J. Activated Carbons Prepared from Kraft Lignin by Phosphoric Acid Impregnation. In *Proceedings of Carbon 2003*, Oviedo, Spain, July 6−10, 2003.
(11) Ahmadpour, A.; Do, D. D. The preparation of active carbons from coal by chemical and physical activation. *Carbon* **1996**, *34*, 471–479.
(12) Frackowiak, E.; Beguin, F. Electrochemical storage of energy in carbon nanotubes and nanostructured carbons. *Carbon* **2002**, *40*, 1775–1787.
(13) Liang, C.; Wei, Z.; Xin, Q.; Li, C. Ammonia synthesis over Ru/C catalysts with different carbon supports promoted by barium and potassium compounds. *Appl. Catal., A* **2001**, *208*, 193–201.
(14) Otowa, T.; Nojima, Y.; Miyazaki, T. Development of KOH activated high surface area carbon and its application to drinking water purification. *Carbon* **1997**, *35*, 1315–1319.
(15) Fierro, V.; Torné-Fernández, V.; Celzard, A. Highly microporous carbons prepared by activation of Kraft lignin with KOH. *Stud. Surf. Sci. Catal.* **2005**, 607–614.
(16) Azargohar, R.; Dalai, A. K. Production of activated carbon from Luscar char: experimental and modeling studies. *Microporous Mesoporous Mater.* **2005**, *85*, 219–225.
(17) Bacaoui, A.; Dahbi, A.; Yaacoubi, A.; Bennouna, C.; Maldonado-Hodar, F. J.; Rivera-Utrilla, J.; Carrasco-Marin, F.; Moreno-Castilla, C. Experimental design to optimize preparation of activated carbons for use in water treatment. *Environ. Sci. Technol.* **2002**, *36*, 3844–3849.
(18) Goel, J.; Kadirvelu, K.; Rajagopal, C.; Garg, V. K. Removal of mercury(II) from aqueous solution by adsorption on carbon aerogel: response surface methodological approach. *Carbon* **2005**, *43*, 197–200.
(19) Karacan, F.; Ozden, U.; Karacan, S. Optimization of manufacturing conditions for activated carbon from Turkish lignite by chemical activation using response surface methodology. *Appl. Therm. Eng.* **2007**, *27*, 1212–1218.
(20) Ravikumar, K.; Deebika, B.; Balu, K. Decolourization of aqueous dye solutions by a novel adsorbent: application of statistical designs and surface plots for the optimization and regression analysis. *J. Hazard. Mater.* **2005**, *122*, 75–83.
(21) Ravikumar, K.; Krishnan, S.; Ramalingam, S.; Balu, K. Optimization of process variables by the application of response surface methodology for dye removal using a novel adsorbent. *Dyes Pigm.* **2007**, *72*, 66–74.
(22) Ravikumar, K.; Pakshirajan, K.; Swaminathan, T.; Balu, K. Optimization of batch process parameters using response surface methodology for dye removal by a novel adsorbent. *Chem. Eng. J.* **2005**, *105*, 131–138.
(23) Ravikumar, K.; Ramalingam, S.; Krishnan, S.; Balu, K. Application of response surface methodology to optimize the process variables for reactive red and acid brown dye removal using a novel adsorbent. *Dyes Pigm.* **2006**, *70*, 18–26.
(24) Veglio, F.; Beolchini, F. Removal of metals by biosorption: a review. *Hydrometallurgy* **1997**, *44*, 301–316.
(25) El-Hendawy, A.-N. A. Surface and adsorptive properties of carbons prepared from biomass. *Appl. Surf. Sci.* **2005**, *252*, 287–295.
(26) Fierro, V.; Torné-Fernández, V.; Celzard, A. Kraft lignin as a precursor for microporous activated carbons prepared by impregnation with *ortho*-phosphoric acid: synthesis and textural characterisation. *Microporous Mesoporous Mater.* **2006**, *92*, 243–250.
(27) Girgis, B. S.; Yunis, S. S.; Soliman, A. M. Characteristics of activated carbon from peanut hulls in relation to conditions of preparation. *Mater. Lett.* **2002**, *57*, 164–172.
(28) Khezami, L.; Chetouani, A.; Taouk, B.; Capart, R. Production and characterisation of activated carbon from wood components in powder: cellulose, lignin, xylan. *Powder Technol.* **2005**, *157*, 48–56.
(29) Lei, S.; Miyamoto, J.-I.; Kanoh, H.; Nakahigashi, Y.; Kaneko, K. Enhancement of the methylene blue adsorption rate for ultramicroporous carbon fiber by addition of mesopores. *Carbon* **2006**, *44*, 1884–1890.
(30) Stavropoulos, G. G. Precursor materials suitability for super activated carbons production. *Fuel Process. Technol.* **2005**, *86*, 1165–1173.
(31) Stavropoulos, G. G.; Zabaniotou, A. A. Production and characterization of activated carbons from olive-seed waste residue. *Microporous Mesoporous Mater.* **2005**, *82*, 79–85.
(32) Torné-Fernández, V.; Fierro, V.; Mateo, J. M.; Celzard, A. Highly Microporous Carbons from Chemical Activation of Lignin with Hydroxides: Optimization of Preparation Conditions. Proceedings of the 10th Mediterranean Congress of Chemical Engineering, Barcelona, Spain, Nov 15−18, 2005.
(33) Tseng, R.-L.; Tseng, S.-K. Pore structure and adsorption performance of the KOH-activated carbons prepared from corncob. *J. Colloid Interface Sci.* **2005**, *287*, 428–437.
(34) Warhurst, A. M.; McConnachie, G. L.; Pollard, S. J. T. Characterisation and applications of activated carbon produced from *Moringa oleifera* seed husks by single-step steam pyrolysis. *Water Res.* **1997**, *31*, 759–766.
(35) Wu, F.-C.; Tseng, R.-L.; Hu, C.-C. Comparisons of pore properties and adsorption performance of KOH-activated and steam-activated carbons. *Microporous Mesoporous Mater.* **2005**, *80*, 95–106.
(36) Wu, F.-C.; Tseng, R.-L.; Juang, R.-S. Pore structure and adsorption performance of the activated carbons prepared from plum kernels. *J. Hazard. Mater.* **1999**, *69*, 287–302.
(37) Wu, F.-C.; Tseng, R.-L.; Juang, R.-S. Comparisons of porous and adsorption properties of carbons activated by steam and KOH. *J. Colloid Interface Sci.* **2005**, *283*, 49–56.
(38) Fierro, V.; Torné-Fernández, V.; Celzard, A.; Montané, D. Influence of the demineralisation on the chemical activation of Kraft lignin with orthophosphoric acid. *J. Hazard. Mater.* **2007**, *149*, 126–133.
(39) Montgomery, D. C. *Design and Analysis of Experiments*, 5th ed.; John Wiley & Sons: New York, 2000.
(40) Prat, A.; Tort-Martorell, X.; Pozueta, L. *Métodos Estadísticos: Control y Mejora de la Calidad*; UPC: Barcelona, Spain, 1997.
(41) Rouquerol, F.; Rouquerol, J.; Sing, K. S. W. *Adsorption by Powders and Porous Solids: Principles, Methods, and Applications*; Academic Press: San Diego, CA, 1999.
(42) Setoyama, N.; Suzuki, T.; Kaneko, K. Simulation study on the relationship between a high resolution [alpha]s-plot and the pore size distribution for activated carbon. *Carbon* **1998**, *36*, 1459–1467.
(43) Kruk, M.; Li, Z.; Jaroniec, M.; Betz, W. R. Nitrogen adsorption study of surface properties of graphitized carbon blacks. *Langmuir* **1999**, *15*, 1435–1441.
(44) Boehm, H. P. Chemical identification of surface groups. *Adv. Catal.* **1966**, *16*, 179–225.
(45) Fierro, V.; Torné-Fernández, V.; Celzard, A. Methodical study of the chemical activation of Kraft lignin with KOH and NaOH. *Microporous Mesoporous Mater.* **2006**, *101*, 419–431.
(46) Guo, Y. P.; Qi, J. R.; Yang, S. F.; Yu, K. F.; Wang, Z. C.; Xu, H. D. Adsorption of Cr(VI) on micro- and mesoporous rice husk-based active carbon. *Mater. Chem. Phys.* **2002**, *78*, 132–137.
(47) Guo, Y. P.; Yang, S. F.; Fu, W. Y.; Qi, J. R.; Li, R. Z.; Wang, Z. C.; Xu, H. D. Adsorption of malachite green on micro- and mesoporous rice husk-based active carbon. *Dyes Pigm.* **2003**, *56*, 219–229.
(48) Guo, Y. P.; Yang, S. F.; Yu, K. F.; Zhao, J.; Wang, Z. C.; Xu, H. D. The preparation and mechanism studies of rice husk based porous carbon. *Mater. Chem. Phys.* **2002**, *74*, 320–323.
(49) Guo, Y. P.; Yu, K. F.; Wang, Z. C.; Xu, H. D. Effects of activation conditions on preparation of porous carbon from rice husk. *Carbon* **2000**, *41*, 1645–1648.
(50) Lillo-Rodenas, M. A.; Cazorla-Amoros, D.; Linares-Solano, A. Understanding chemical reactions between carbons and NaOH and KOH. An insight into the chemical activation mechanisms. *Carbon* **2003**, *41*, 267–275.
(51) Amarasekera, G.; Scarlett, M. J.; Mainwaring, D. E. Development of microporosity in carbons derived from alkali digested coal. *Carbon* **1998**, *36*, 1071–1078.
(52) Pereira, M. F. R.; Soares, S. F.; Orfao, J. J. M.; Figueiredo, J. L. Adsorption of dyes on activated carbons: influence of surface chemical groups. *Carbon* **2003**, *41*, 811–821.

Received for review November 5, 2008. Accepted April 24, 2009. Funding for this work was provided by the Spanish Ministry of Science and Technology (MCYT, project PPQ2002-04201-CO2-02, partially funded by the FEDER program of the European Union) and the Catalan Regional Government (project 2005SGR-00580). V.T.-F. acknowledges the URV for her Ph.D. grant.

JE800827N